

---

# Improvement of parallel efficiency of particle-based simulations on present and near-future large-scale parallel computers

Masaki IWASAWA<sup>1</sup>, Long WANG<sup>2,1</sup>, Keigo NITADORI<sup>1</sup>, Daisuke NAMEKATA<sup>1</sup>,  
Miyuki TSUBOUCHI<sup>1</sup>, Junichiro MAKINO<sup>3,1,4</sup>, Zhao LIU<sup>5</sup>, Haohuan FU<sup>6,5</sup> and  
Guangwen YANG<sup>7,6,5</sup>

<sup>1</sup>RIKEN Advanced Institute for Computational Science

<sup>2</sup>Helmholtz Institut für Strahlen und Kernphysik

<sup>3</sup>Department of Planetology, Graduate School of Science, Kobe University

<sup>4</sup>Earth-Life Science Institute, Tokyo Institute of Technology

<sup>5</sup>National Supercomputing Center in Wuxi

<sup>6</sup>Ministry of Education Key Lab. for Earth System Modeling, and Department of Earth System Science, Tsinghua University

<sup>7</sup>Department of Computer Science and Technology, Tsinghua University

\*E-mail: masaki.iwasawa@riken.jp, long.wang@riken.jp, keigo@riken.jp, daisuke.namekata@riken.jp, miyuki.tsubouchi@riken.jp, makino@mail.jmlab.jp, liuzhao@mail.nscwx.cn, haohuan@tsinghua.edu.cn, ygw@tsinghua.edu.cn

Received ; Accepted

## Abstract

In this paper, we describe several new algorithms we developed for large-scale particle-based simulations on present and near-future large-scale HPC systems. It has become more and more difficult to achieve high efficiency on many of numerical simulations on modern HPC systems, for a variety of reasons. We can summarize the reasons as (a) very large number of computing cores, exceeding  $10^7$  on recent machines, (b) relatively low main memory bandwidth, (c) even lower network bandwidth, and in some cases (d) communication bottleneck between general-purpose CPUs and “accelerator”. Historically, the efficiency achieved with

$N$ -body simulations on high-end HPC systems has been pretty high, such as more than 50% of the theoretical peak speed. However, on some of precent or planned architecture, even the best parallel implementation, after careful performance tuning, would achieve less than 5%. In this paper, we analyse the reason for such low efficiency and propose a combination of new algorithms designed to improve the performance of  $N$ -body simulations on modern HPC systems. New algorithms can be divided into three categories. Algorithms of the first category are designed to reduce the calculation cost of the part other than the pure interaction calculation. Those in the second category are designed to reduce communication between processes, and those in the third category are optimization specific to the geometry of the physical system. We have implemented these new algorithms to FDPS (Framework for Developing Particle Simulators) and measured the performance on Sunway TaihuLight. We achieve 3.83 Pflops, or 31 % of the theoretical peak on 16384 processes (4096 nodes), when we use 16G particles. We plan to use this code for the study of global dynamics of rings. The generic version of the code is publicly available.

**Key words:** Methods: numerical — Galaxy: evolution — Cosmology: dark matter — Planets and satellites: formation

---

## 1 Introduction

In this paper, we describe the new algorithms we implented to FDPS (Framework for Developing Particle Simulators, [ref here]). FDPS is designed to make it easy for many researchers to develop his/her own programs for particle-based simulations. To develop efficient parallel programs for particle-based simulations requires a very large amount of work, like the work of a large team of people for many years. This is of course true not only for the particle-based simulations, but practically for any field of computational science. The main reason is that the modern HPC (high-performance computing) platforms have become very complex, and thus requires lots of efforts to develop complex programs to make efficient use of such platforms.

Typical modern HPC systems are actually a cluster of computing nodes connected through a network, each with typically one or two processor chips. Largest systems at present consists of around  $10^5$  nodes, and we will see even larger systems soon. This extremely large number of nodes makes the design of inter-node network very difficult, and the design of parallel algorithm also becomes very difficult. We need to make very precise balance for the calculation times of all nodes, and we

need to make the time necessary for communication small enough so that the use of large systems is meaningful. The communication bandwidth between nodes is much lower than the main memory bandwidth, which itself is very small compared to the calculation speed of CPUs. Thus, it is crucial to avoid communications as much as possible. It can easily happen that calculation time would show increase, instead decrease, when we use a large number of nodes.

In addition, the programming environment available on present-day parallel systems is very poor. What is most widely used is MPI, in which we need to write the program for a single node, instead of expressing what should be done for the entire physical system we are dealing with. We also need to write explicitly how each node communicates with all others in the system. Just to write and debug the program is difficult, and it has become nearly impossible for any single person or even for a group of people to develop large-scale simulation programs which run efficiently on modern HPC systems.

Moreover, this extremely large number of nodes is just one of the many serious difficulties in using modern HPC systems, since within one node, there are many other levels of parallelisms which should be taken care of by programmers. To make the matter even more complicated, these multiple levels of parallelism are interwoven with multiple levels of memory hierarchy with varying bandwidth and latency. For example, the “post-K” computer, which is under development in Japan as of the time of writing, will have 48 CPUs (cores) in one chip. These 48 cores are divided into four groups, each with 12 cores. Cores in one group share the level-2 cache memory. The cache memories in different groups communicate with each other through cache-coherency protocol. Thus, the access of one core to the data which happens in its level-2 cache is fast, but that in the cache of other groups can be very slow. Also, the access to the main memory is much slower, and that to local level-1 cache is much faster. Thus, we need to take into account the number of cores and the size and speed of caches at each level to extract an acceptable performance. To make the matter worse, many of modern microprocessors have level-3 or even level-4 caches.

As the result of these difficulties, only a small number of researchers (or groups of researchers) can develop their own simulation programs. In the case of cosmological and galactic  $N$ -body and SPH simulations, Gadget (ref) and pkdgrav (ref) are most widely used. For star cluster simulations, NBODY6++ (and NBODY6++GPU) is effectively the standard. For planetary ring dynamics, REBOUND has been available. There has been no public code for simulations of planetary formation process until recently.

This situation is clearly unhealthy. In many cases, the physics need to be modeled is quite simple: particles interact through gravity, and with some other interactions such as physical collisions. Even so, almost all researchers are now forced to use existing programs developed by someone else,

simply because HPC platforms have become too difficult to use. To add some functionality which is not already implemented in existing programs can be very difficult.

In order to make it possible for researchers to develop their own parallel codes for particle-based simulations, we have been developing FDPS (Framework for Developing Particle Simulators, [ref here]).

The basic idea of FDPS is to separate the code for parallelization and that for interaction calculation and numerical integration. FDPS provides the library functions necessary for parallelization, and using them researchers write programs very similar to what they would write for single CPU. Parallelization using MPI and on multiple cores in single node are taken care of by FDPS.

FDPS provides three sets of functions. One is for the domain decomposition. Given the data of particles on each node, FDPS constructs the decomposition of the computational domain. These domains are assigned to MPI processes. The second one is to send particles to the computing nodes according to their coordinate. Each particle should be sent to the appropriate MPI process with domain in which it exists. The third set of functions perform the interaction calculation. FDPS uses parallel version of Barnes-Hut algorithm, for both of long-range interactions such as gravitational interactions and short-range interactions such as intermolecular force or SPH interaction. Application program gives the function to perform interaction calculation for two groups of particles (one group exerting force to another), and FDPS calculates the interaction using that function.

FDPS offers very good performance on large-scale parallel systems consisting of “homogeneous” multi-core processors, such as K computer (ref) and Cray systems based on x86 processors. On the other hand, the architecture of large-scale HPC systems have been shifting from homogeneous multi-core processors to accelerator-based systems and heterogeneous multi-core processors.

GPGPUs are most widely used accelerators, and are available on many large-scale systems. They offer the price-performance ratios and performance per watt numbers significantly better than those of homogeneous systems, primarily by integrating a large number of relatively simple processors on single accelerator chip. On the other hand, Accelerator-based systems have two problems. One is that for many applications, the communication bandwidth between the CPU and the accelerator becomes the bottleneck. The second one is that because the CPU and the accelerator have separate memory spaces, the programming becomes complex and we cannot use existing programs.

Though in general it is difficult to use accelerators, for particle-based simulations the efficient use of accelerators is not very difficult, and that fact is the reason why GRAPE families of accelerators specialized for gravitational  $N$ -body simulations had been successful (ref). GPGPUs also are widely used both for collisional (ref) and collisionless (ref) gravitational  $N$ -body simulations. Thus, it is clearly necessary for FDPS to support accelerator-based architectures.

Heterogeneous many-core architecture is not yet very popular, but expected to become popular. In a processor with heterogeneous many-core architecture, complex and powerful CPU cores and much simpler accelerator-like cores are integrated. Heterogeneous many-core architecture “solves” the two main problems of accelerator-based architecture we described above, since there is no communication bottleneck between CPU cores and accelerator cores, and they share the same memory space.

As of March 2018, the fastest supercomputer in the world, Sunway TaihuLight, is equipped with processors with heterogeneous many-core architecture, and the fourth, GYOKOU system, also equipped with processors with heterogeneous many-core architecture.

These systems with heterogeneous architecture, though in principle have “solved” the problems of accelerator-based systems, in practice require new approaches to achieve high efficiency. There are several reasons why new approaches are necessary

1. The CPU cores are usually relatively weak.
2. The main memory bandwidth is low compared to the performance of the accelerator cores.
3. The inter-node network is relatively weak.
4. Programming environment is poor or cannot extract the performance of hardware.

The first three reasons come simply from the fact that accelerator cores are much faster than the CPU cores for the same silicon area and power consumption. In addition, in order to achieve good performance, we need to minimize the power and silicon area spent for CPU cores. As a result, all other components look slower compared to accelerator cores. As we stated above, even in the case of homogeneous manycore systems, main memory and networks are much slower compared to CPUs. With heterogeneous systems this problem becomes much more severe.

Recently, a number of new findings have been made on the dynamics of the rings of Saturn, primarily through the Cassini mission. Among the new findings, probably the most surprising is that the rings show dynamic changes of structures, possibly including the formation of new satellites. Another example of truly new findings of the Cassini mission is the vertical structure at the outer edge of the B ring. (references necessary here)

For some of these new findings, theoretical explanation based on fluid approximation has been made. However, many of them cannot be explained by simple fluid models, and more realistic treatment of ring as collection of particles interacting through both mutual gravity and physical collisions is necessary.

Planetary rings are usually at the radii around the Roche limit. Thus, mutual gravity between particles does not easily lead to the formation of new satellites. However, spiral waves (“wakes”)

in very small scales can be formed through self-gravity, and it increases the effective viscosity and enhances the radial transport of the angular momentum. On the other hand, the actual ring system seems to consist of very large number of very narrow rings, separated with distinct gaps. It has been believed that high-order resonances with small embedded satellites (so-called moonlets) form these gaps, but this belief lacks observational/theoretical support.

Very little simulation-based studies have been done to understand these new findings. The primary reason for this lack is simply that simulations of such structures must be global simulations including self gravity of ring particles, which would require very large number of particles and thus very large amount of computing resources.

Up to now, most of simulations of ring structures have been local ones, in which a small patch was cut out from the ring and simulated under the assumption of the local Hill approximation and periodic boundary condition (Wisdom & Tremaine 1988). Rein & Latter (2013) performed “Large-scale” simulation of viscous overstability in Saturn’s rings, using up to 204,178 particles and up to 10,000 orbits using this local approach. Because very long simulations are necessary, the number of particles has been small. They used REBOUND (Rein & Liu 2012), an MPI-parallel  $N$ -body simulation code. More recently, Ballouz et al. (2017) used pkdgrav(Stadel 2001) for simulations with up to 500k particles.

Compared to the size of local simulations performed so far, the number of particles necessary for global simulations might seem too large. However, such large simulations are not beyond the reach of present-day supercomputers.

We have developed a framework for developing fast and highly scalable codes for particle-based simulations, FDPS (Framework for Developing Particle Simulator) (Iwasawa et al. 2016). Using FDPS, Michikoshi & Kokubo (2017) performed global simulations of rings with probably the largest number of particles. They used 300M particles to model two narrow rings of Chariklo and followed the system for 10 orbital period. The number of particles they used is already three orders of magnitude larger than what have been used for global simulations. They have used Cray XC30 at the Center of Computational Astrophysics, National Astronomical Observatory of Japan, with the peak speed of 1 Pflops. In order to model fine structures of Saturn’s rings, we need to increase the number of particles by another three orders of magnitude.

The total calculation cost is roughly proportional to number of particles multiplied by the number of orbital periods followed, since the calculation cost per timestep is  $O(N \log N)$  when Barnes and Hut tree algorithm (Barnes & Hut 1986) is used and the number of timestep required for ring simulations is essentially independent of the number of particles. Thus, we can conclude that the size of state-of-the-art simulations of planetary rings is around  $3 \times 10^9$  particle-orbits, or around  $3 \times 10^{12}$

particle-steps.

We should note that even though the simulations so far done in this field is relatively small, that does not mean there is no need or possibilities for larger scale simulations. If we want to model the global structures of rings, we cannot rely on local treatment. For example, the effect of resonances with small satellites can only be studied using global simulations. On the other hand, the number of particles one needs for global simulations, even for a very narrow radial range, is very large. For example, consider A ring of Saturn with the radius of around  $1.3 \times 10^5$  km. The typical radius of ring particles is 6 m (Zebker et al. 1985), and the optical depth of the ring is around unity. Thus, we need  $10^4$  particles per  $\text{km}^2$  or around  $10^{12}$  particles for the radial range of 100 km. With this radial range, we can model many of fine features observed by Cassini directly.

If we could use particles with larger size, we could reduce the number of particles required significantly. However, that would change the viscous diffusion timescale of the ring, and thus what would be observed. Thus, if at all possible, it is desirable to perform simulations with particle of real physical radius, which would require at least  $10^{16}$  and ideally  $10^{19}$  particle-steps.

In other fields of astrophysics, very large simulations have been performed. For example, Ishiyama (2014) used  $4096^3$  particles to follow the formation and growth of dark matter halos of smallest scales. This simulation corresponds to  $10^{16}$  particle-steps. Part of this calculation was performed on K computer. The performance of K computer is  $4.0 \times 10^{10}$  particle-steps per second on the entire K computer, or 60,000 particle-step per second per core for a processor core with the theoretical peak performance of 16 Gflops (Ishiyama et al. 2012). The efficiency they achieved is 55% of the theoretical peak.

Bédorf et al. (2014) performed the simulation of Milky Way Galaxy using  $2.42 \times 10^{11}$  particles on large-scale GPGPU clusters. The achieved performance is 24.77 Pflops on ORNL Titan, and one timestep took 5.5 seconds. Thus they have achieved the performance of  $4.4 \times 10^{10}$  particle-steps per seconds. The theoretical peak performance of Titan is 73.2 Pflops in single precision. Thus, the achieved efficiency is 33.8%.

The current super computers are powerful enough to perform a realistic global ring simulation. Thus we are trying to revile the mechanisms of formation and evolution of ring structures of the Saturn using the global ring simulation.

As a first step of the investigation of the ring dynamics, we propose efficient algorithms of global ring simulations and implement them to FDPS. To develop the algorithms we use Sunway TaihuLight which is the first ranked on the top 500 list on Nov. 2017. Its processor (SW26010) is heterogeneous many-core archetecture. However, since our algorithms are not specialized for heterogeneous manycore archetecture based system, they are also useful for other manycore archetecture

based systems or single- or multi-core CPU based systems.

In this paper, we report new efficient algorithms for the global planetary ring simulations and the measurement of its performance on Sunway TaihuLight. The paper is organized as follows. In section 2, we briefly describe manycore systems, especially the features of the Sunway TaihuLight system and its SW26010 processor. In section 3, we briefly review the original implementation of FDPS and the problems with the planetary ring simulation on TaihuLight. In section 4, we describe the algorithms we developing. In section 5, we present the measured performance on TaihuLight. In section 6, we summarize the results.

## 2 Manycore System

Recently, super computers installing manycore processors, such as SW26010, GPU (graphics processing unit), Xeon-Phi and PEZY-SC are widely used in the field of HPC. For example, in Nov. 2008 only one manycore system was on the top 500 list, but in Nov. 2017, about 100 systems have manycore processors on the list. Especially, eight systems in top 10 have manycore processors in Nov. 2017.

One reason of the increase of using manycore porcessors is low power consumption of many-core processors compared to single- or multi- core processors. Power consumption of super computers have become a issue over ten years, in the point of view of running cost and enviromental protection. Thus manycore systems would become more inportant in the field of HPC.

Sunway TaihuLight system is one of the manycore systems. It consists of 40960 nodes, connected by the network with injection bandwidth of 8GB/s per node. The hardware network bandwidth is large enough for our purpose.

The processor itself consists of four CGs (core groups), each with one MPE (management processing element) and 64 CPEs (computing processing elements). Both MPE and CPE are 64-bit RISC cores. MPE has L1 cache memories for both instructions and data, and also L2 data cache. On the other hand, each CPE has L1 instruction cache and 64KB of local data memory. CPEs can communicate with the main memory through DMA. Each CPE can initiate multiple asynchronous DMA operations. Thus, it is possible to write the kernel loop so that the computation, DMA read for the data which will be necessary for the next iteration, and DMA write operation of the result of the previous iteration all run concurrently and thus the communication with the main memory is completely hidden. This capability of explicit control of communication with main memory is crucial for achieving high efficiency.

Each core group is connected to 8GB DDR3 DRAM with the theoretical peak transfer rate of



34GB/s. The processor runs at the clock frequency of 1.45GHz, and each core (both MPE and CPE) can perform four double precision FMA operations. Thus, the theoretical peak performance of one processor is 3016 Gflops and that of one CG is 754 Gflops.

CPEs in one CG are organized into an  $8 \times 8$  array, and within each row or column, low-latency, high-bandwidth point-to-point and broadcast communications are supported.

Operating system runs on MPE, and by default the user program also runs on MPE. In order to use CPEs, there are two ways. One is to use an extension of OpenACC designed for SW26010 processor, and the other is use a lightweight thread library called Athread. Athread is more difficult to use compared to OpenACC, but allows fine-grained control of CPEs.

### 3 Problems of Original FDPS Implementation on TaihuLight

In this section, we describe the original implementation of FDPS and problems we would encounter if we use original FDPS on TaihuLight.

The following gives the steps for parallel Barnes-Hut tree code when using FDPS on CPU-based super computer.

1. Perform domain decomposition by the multisectin method (Makino 2004).
2. Exchange particles so that particles belong to appropriate domains.
3. Construct the “local” tree structure from particles in the domain.
4. Calculate physical quantities of the tree cell of the local tree.
5. Exchange the information necessary for the calculation of interaction from other processes [so called local essential tree (LET)].
6. Construct the “global” tree from the collected information.
7. Calculate physical quantities of the tree cell of the global tree.
8. For small group of particles, construct the interaction list during traverse the tree.
9. Calculate interactions on the particles from particles in the interaction list.
10. Repeat steps 8 and 9 until the calculation of forces on all particles is completed.
11. Integrate the orbits of particles.
12. Go back to step 1.

For GPUs, FDPS version 2.0 or later also adopt the extension of this algorithm, in which multiple pairs of particle groups and lists are constructed and then passed to GPU (Hamadaetal 2009). In this algorithm, all computations, except for the actual interaction calculation in the double loop, is done on general-purpose front-end computer. During the interaction calculation on GPGPUs, the front-end computer constructs the next interaction lists. Thus we can hide constructing interaction

list.

If we use this algorithms on Sunway TaihuLight, CPEs are used only for interaction calculations and the other parts are done on MPEs. However, this algorithm is not sufficient on Sunway TaihuLight. This is simply because MPE is too slow compared with CPEs. The execution time for MPE to perform the tree construction and tree traversal is more than 10 times longer than that for CPEs to do the interaction calculation, if the efficiency of the interaction kernel is reasonably high 30-50%. The same problem would occur even if we use CPU-GPU heterogeneous systems with the performance ratio of CPU to GPU is large. Bédorf et al. (2014) avoid this problem by porting all procedures to GPU side. However, even when this approach is adopted, getting reasonable efficiency turned out to be not easy, since then the performance of tree construction and tree traversal would be limited by the bandwidth of the main memory for random access. Thus, traditional approach for Barnes-Hut tree algorithm is not sufficient for manycore processors.

Thus, it is necessary to introduce some new approach to reduce the calculation (or main memory access) cost of operations other than the interaction calculation. We adopted the neighbor-list method used in molecular-dynamics simulations with short-range interactions, in which the list constructed before is persistently used for multiple steps (hereafter we call this method persistent-list method). In next section, we will describe this method.

## **4 New Algorithms for Planetary Ring Simulation on Manycore System**

In this section, we describe new algorithms for simulating self-gravitating planetary ring on manycore system, such as TaihuLight.

### **4.1 Persistent List Method**

In the global ring simulations, each particle moves on nearly circular orbit and a logical structure of the tree is almost the same for a shear time scale of the ring. Thus we can persistently use the same tree structure and interaction lists for multiple timesteps.

By using the same interaction list persistently, we can reduce the calculation cost of the part other than the interaction calculation drastically. While we are using the same interaction list, we skip the domain decomposition, exchange of particles, construction of the local tree. We still need to update the physical quantities of the cells of the local tree, since particles in the lowest level have moved. Then, using the list of tree cells for the local essential tree, the communication between the processes is performed. Finally, the physical quantities of the global tree is updated, and the force calculation is performed using this updated global tree and the persistent interaction list.

The steps of persistent list method is as follows.

1. Perform domain decomposition by the multisection method.
2. Exchange particles so that particles belong to appropriate domains.
3. Construct the “local” tree structure from particles in the domain.
4. Calculate physical quantities of the tree cell of the local tree.
5. Exchange LETs and memorize them and their destination and source processes.
6. Construct the “global” tree from the collected information.
7. Calculate physical quantities of the tree cell of the global tree.
8. For small group of particles, construct the interaction list and memorize it during traverse the tree.
9. Calculate interactions on the particles from particles in the interaction list.
10. Repeat steps 8 and 9 until the calculation of forces on all particles is completed.
11. Integrate the orbits of particles.
12. Calculate physical quantities of the tree cell of the local tree.
13. Exchange LETs memorized at step 5.
14. Calculate physical quantities of the tree cell of the global tree.
15. Calculate interactions on the particles from particles in the interaction list.
16. Integrate the orbits of particles.
17. Go back to step 12 until the interaction list is expired.
18. Go back to step 1.

We should note that FDPS memorize not only the interaction list, but also LETs and their destination and source processes at step 5. In other words, we can skip the tree traversal for constructing LETs and the communication of exchanging the number of LETs among all processes.

#### 4.2 Tree and Domain Structures on Cylindrical Coordinate

In original implementation, a logical structure of the tree cells and computational domains are calculated on a Cartesian coordinate. However, the Cartesian coordinate is not suitable for the global planetary ring simulations. We can see this reason from Figure 1 which gives an example of domain decomposition by  $32 \times 16$  on the Cartesian coordinate for a quadrant of a ring with the radius of 1.0 and the width of 0.1.

Domains have various shape and some of them have high aspect ratio. The domains at  $x \sim 0$  are elongated along the x direction. On the other hand, the domains at  $x \sim 1$  are elongated along the y direction. However, the domain shapes at  $x \sim 0$  and  $x \sim 1$  are not 90-degree rotation symmetric.

The wide variation of the domain shapes means that tree structure and the length of the inter-

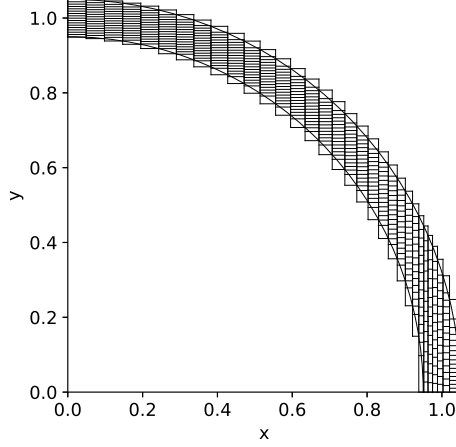


**Fig. 1.** Schematic figure of domain decomposition by the multisection method in x-y coordinate. Domains are divided by 32x16.

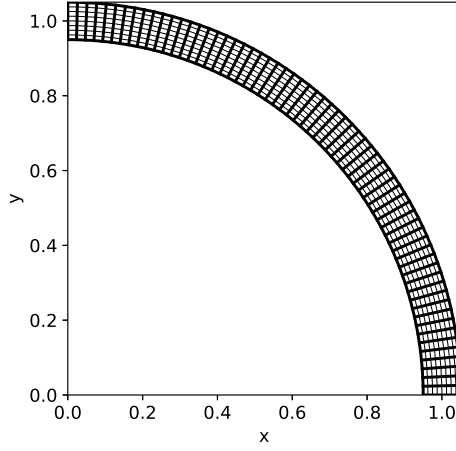


**Fig. 2.** Schematic figure of domain decomposition by the multisection method in cylindrical coordinate. Domains are divided by 8x64. Large boxes with thick curves indicate super domains (see in section 4.4)

action list are the largely different for different processes. Thus it is difficult to achieve a good load balance. In addition, the high aspect ratio of the domain increases the communication costs, because the costs is roughly proportional to the area of the surface of the domain.

In the point of view of the load balance and communication cost, the ideal case is that the shapes of all domains are the same squares. Unfortunately, as long as we use the Cartesian coordinate, the ideal decomposition is difficult because of the curvature of the ring.

To approach the ideal domain decomposition, we introduce a cylindrical coordinate  $(r, \phi, z)$ . We replace  $x$  and  $y$  with  $\phi$  and  $r$ . In this coordinate, a distance between two separate points  $ds$  can be approximated by

$$ds^2 = dx^2 + dy^2 + dz^2 \sim d\phi^2 + dr^2 + dz^2, \quad (1)$$

where we assume that the average ring radius is unity.

Figure 2 is the same as figure 1, but decomposed by  $8 \times 64$  by using the cylindrical coordinate. Each domains have almost the same square shapes. It means the good load balance and the decreasing communication costs compared to those on the Cartesian coordinate.

We also introduce this coordinate to the tree structure: We evaluate opening angle of tree cells with the cylindrical coordinate for constructing the tree, LET and the interaction lists. On the other hand, for the calculation of the multiple moment of the tree cell and the interaction calculation, we use the position defined by the Cartesian coordinate.

For large  $\phi$ , the approximation of equation 1 is broken and the distance is overestimated. For example, at  $\phi = \pi$ , the approximation distance is overestimated by 57 %. This approximation means that the accuracy of the force evaluated by multipole approximation from distant particles is somewhat worse. However, since the ring system is roughly one-dimensional structure, the contributions from distant tree cell decreases as  $\phi^{-1}$ . Thus our approximation dose not cause serious problem.

#### 4.3 Counter Rotation of Particles for Exchange Particles

Before the construction of the local tree, particles should migrate so that they belong to appropriate domains. In a reference rest-frame, the particle move a large distance for multiple timesteps. It means most particles should go to other domains. It could increase the communication cost. However, in a rotating frame with the typical angular speed of the ring, most particles do not seem to move a large distance. Thus, before the exchange particle, we can reduce the communication costs by counter-rotating particles by the same angle as the typical rotation angle of the ring.

#### 4.4 Super Domain to Remove All-to-All Communication for Exchange LETs

In the original implementation of the exchange LET, each domain measure the distances from all other domains and exchange LETs among all processes. This communication is realized by `MPI_Alltoall(v)`.

Figures 3 and 4 show the wall clock times of `MPI_Alltoall` and `MPI_Alltoallv` against the number of processes and the size of the sent message per process, respectively. The wall clock time is almost linear against the number of processors for small number of processes. However, for large number of processes, the time of `MPI_Alltoallv` rapidly increase. From figure 4, the wall clock time of `MPI_Alltoallv` is more than 10 seconds when the number of processes of 16384 for any message size. As we will see later, the execution time of our interaction kernel is less than 300 ms, when we

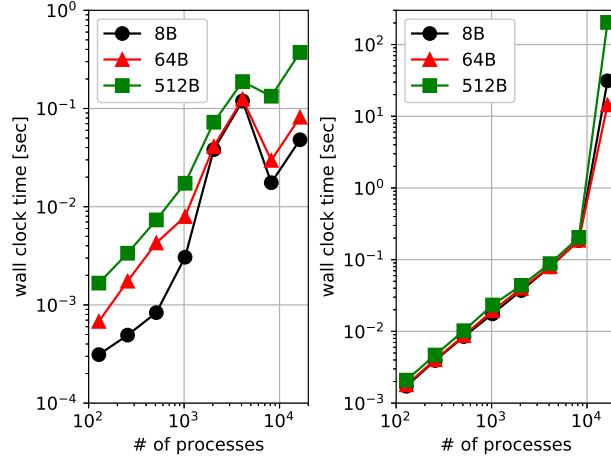


Fig. 3. Wall clock time for MPI\_Alltoall (left) and MPI\_Alltoallv (right) against the number of processes.

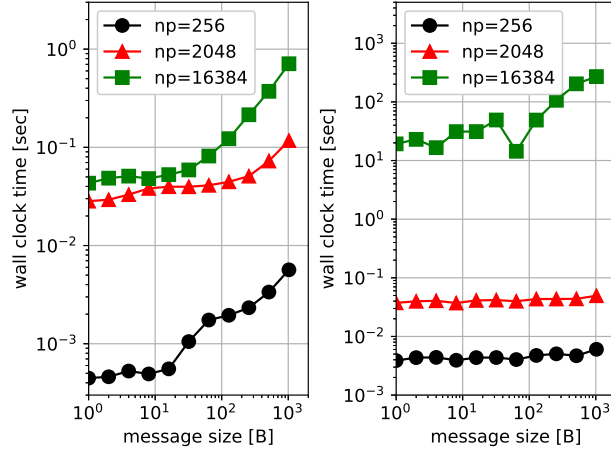


Fig. 4. Wall clock time for MPI\_Alltoall (left) and MPI\_Alltoallv (right) against the size of the message sent per process.

use 1M particles per process. Thus if we use more than  $\sim 2048$  processes, we must avoid to use MPI\_Alltoallv (and also MPI\_Alltoall).

To avoid all-to-all communications, we introduce a kind of tree structure to the domains. In principle, if we have the tree of domains, the all-to-all communication among all processes is not needed because each process does not need the multipole moments from distant domains individually, but only needs locally combined multipole moment from distant domains.

For simplicity, in our method, we adopt the original domain structure by the multisection methods as the tree structure with the depth of two. In other words, the root cell of the domain tree has  $n_\phi$  sub-cells (hereafter, call it “super domain”. see Figure 2) and each sub-cell (“super domain”) has  $n_r$  sub-sub-cells (we do not divide domains in the  $z$  direction because the thickness of the ring is very thin). Here  $n_\phi$  and  $n_r$  are the number of processes in the  $\phi$  and  $r$  directions, respectively.

The steps of the exchange LET using the super domain is as follows.

1. Each process in a super domain sends the information of its top tree cell, such as the multipole moment and the coordinate of the cell, to the process with the most inner domain in the same super domain (hereafter, call it super process) in  $r$ -direction.
2. Each super process combines the multipole moment from received information.
3. Each super process gathers the combined multipole moments from other super domains by using `MPI_Allgather` in  $\phi$ -direction.
4. Each super process broadcasts the combined multipole moments in  $r$ -direction. Here, all processes have all other super-domain information.
5. Each process measures the distances between own super domain and other super domains.
  - (a1) If the distance is far enough, do nothing because this process already received its combined multipole moments at step 3.
  - (b1) Otherwise, the process makes LETs for the target super domain and sends them to the process with the same process-rank in  $r$ -direction in the target super domain by `MPI_Isend/recv`.
  - (b2) The process broadcast the received LETs in  $r$ -direction.

If we use this methods, we can completely remove `MPI_Alltoall(v)`.

#### 4.5 Load Balancer for interaction calculations

The interactions are calculated on 64 CPEs in parallel. In our implementation, different CPEs read different interaction lists and calculate their interactions. Thus we can avoid reduction of the forces between CPEs.

To achieve a good load balance, the length of the interaction list on CPEs should be the same. However, it is difficult to obtain the optimal solution in a reasonable time. Instead of this, we obtain an approximated solution by the greedy algorithm. Our implementation is as follows.

1. Sort the interaction lists by its length (efficient sort algorithms on manycore system will be described in appendix 2).
2. Assign the first 64 lists on 64 CPEs, one-by-one.
3. Assign the next interaction list on the CPE with the shortest total interaction list.
4. Repeat step 3 until all lists are assigned on CPEs.

Note, at step 3, to find the CPEs with the shortest interaction list, we use binary tree algorithm.

## 5 Performance Results

In this section, we describe the initial ring model, interaction model, numerical method and the measured performance of our code.

### 5.1 Initial Ring Model

As an initial model, we make a ring with the radius of 1.0, the width of 0.01 and the optical depth  $\tau$  of 1.0. All particles are identical and their radii are the same as the Roche radius. We put particles on three layers. We put  $N/3$  particles on a regular grid in the cylindrical coordinate on each layer. The grids are shifted in both radial and azimuthal by half grid size to the grids on neighbor layers. The all particles are on circular orbits.

### 5.2 Interaction Model

In our simulations, since  $\tau$  is unity, the particles collide with each other frequently. Since the radius of the particle is the Roche radius, when the particles collide, the particles rather rebound than gravitational accretion. To handle this nature of collision, we regard a particle as a soft sphere. In this model, we consider not only the gravitational force, but also both a spring and a dashpot forces. Equation 2 gives the definition of the particle-particle interaction.

$$\mathbf{F}_{ij} = \begin{cases} G \frac{m_i m_j}{r_{ij}^3} \mathbf{r}_{ij} & (r_{ij} > r_{\text{coll}}) \\ \left[ G \frac{m_i m_j}{r_{\text{coll}}^3} + \frac{m_j}{m_i + m_j} \left( \kappa \frac{r_{ij} - r_{\text{coll}}}{r_{ij}} + \eta \frac{\mathbf{r}_{ij} \cdot \mathbf{v}_{ij}}{r_{ij}^2} \right) \right] \mathbf{r}_{ij} & (r_{ij} \leq r_{\text{coll}}) \end{cases} \quad (2)$$

with  $\mathbf{r}_{ij} = \mathbf{r}_j - \mathbf{r}_i$ ,  $\mathbf{v}_{ij} = \mathbf{v}_j - \mathbf{v}_i$ ,  $r_{ij} = \|\mathbf{r}_{ij}\|$ . Here,  $\mathbf{F}_{ij}$  is the acceleration particle  $i$  due to particle  $j$ ,  $\mathbf{r}_{ij}$  and  $\mathbf{v}_{ij}$  are the relative position and velocity vectors,  $G$  is the gravitational constant,  $m_i$  is the mass of particle  $i$ ,  $r_{\text{coll}}$  is the distance at which two particles collide, and  $\eta$  and  $\kappa$  are parameters which determine the coefficient of restitution. We chose these parameters so that the coefficient of restitution in radial direction is 0.5.

### 5.3 Numerical Method

We use the Barnes-Hut tree method for interaction calculations using modified FDPS including the algorithms described above. The opening criterion of the tree  $\theta$  is 0.5. The integration method is leap frog with the shared timestep of  $1/128$ . We use the same interaction list for 64 steps.

Over 64 steps, not to miss to detect collisions between particles, we do not apply multipole approximation to neighboring particles within three hill radius. To find neighboring particles, we also use the tree. To do this, each tree cell also have a boundary coordinate defined by the positions and



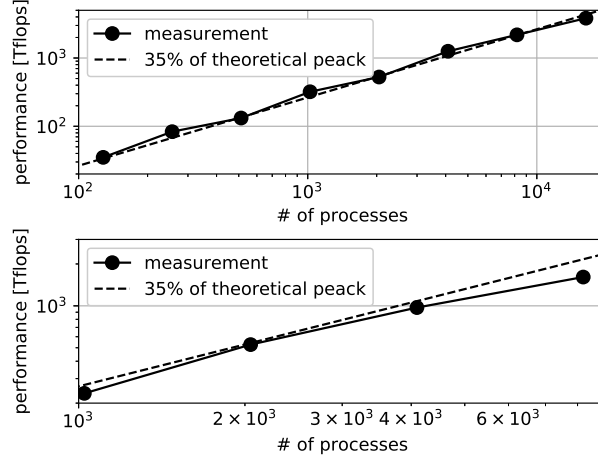


**Fig. 5.** Performance in tera flops for weak-scaling (top) and strong-scaling (bottom) tests. The number of particles per process is 1M for weak-scaling test. For strong-scaling test, the number of particles is 2G. Dashed lines indicate 35 % of the theoretical peak performance of TaihuLight. Closed circles indicate measured performance.

the radius of particles inside the cell.

In the ring simulation the global structure is not drastically changed for rotation period. Thus the domain decomposition is done once at the beginning.

#### 5.4 Performance

To measure the performance, we perform both weak-scaling and strong-scaling tests and measure the time for 64 timesteps. The execution time is measured by the MPI wallclock timer, and operation count is from the counted number of interactions calculated. Particle-particle interaction consists of 9 multiplications, 8 additions, and one square root and one division operations. Instruction set of Sunway 26010 processor does not include fast approximation for neither square root or reciprocal square root. So we implemented fast initial guess and high-order convergence iteration in software. The number of operations in this part is 7 multiplications, 5 additions and two integer operations. Therefore, for particle-cell interactions the number of floating-point operations is 31, and for particle-particle interactions, which include the repulsive force during physical collisions, is 47. We ignore all operations other than the interaction calculation, since as far as the number of floating-point operations is concerned, that for interaction calculation is more than 99% of total operation count.

For the weak-scaling measurement, we have performed runs with 1M particles per MPI process and for the strong-scaling measurement, the total number of particles is 2G.

Figure 5 shows the speed in tera flops, for both the strong and weak scaling measurements. We can see that the weak scaling performance is quite good. The performance of run for 16G particles

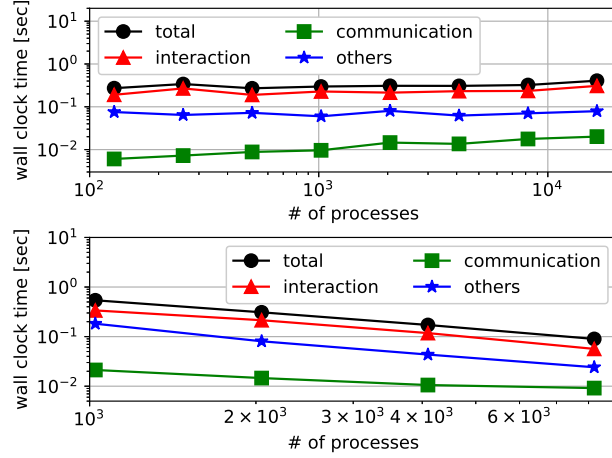


**Fig. 6.** Time per timestep for weak-scaling (top) and strong-scaling (bottom) tests. The number of particles per process is 1M for weak-scaling test. For strong-scaling test, the number of particles is 2G.

on 16384 processes (4096 nodes) is 3.83 PFlops, or 31% of the theoretical peak performance of the Sunway TaihuLight system. The strong scaling performance is not perfectly scaled for large number of processes. However, since our main scientific target is runs with very large number of particles which has been impossible, weak-scaling performance is our main interest.

Figure 6 shows the time per one timestep, for both the strong and weak scaling measurements. The most intensive part is the interaction calculation. The time for communication increase slower than linear increase. This is because we removed `MPI_Alltoall(v)` from the communication parts of FDPS (see Fig. 3 and 4).

Table 1 shows the breakdown in the case of weak-scaling test on 8192 processes. The second and the third column show the time of the first step and the averaged time over 64 steps for each operation. The forth column shows the values in the second column divided by those in the third column. Roughly speaking, these values indicate the speedup factor when we use the persistent list method.

We find that if we use the persistent list method, the total time becomes 5.3 times faster.

The “Local Tree update” and the “Global Tree update” is the time for updating the physical quantities of the tree cell of the local tree and the global tree, respectively. These times become slightly faster. This is because these time include not only the time for calculating multipole moment of the tree cell, but also the time for updating tree cell boundaries. However, the tree cell boundaries is used only for the tree traverse to make interaction lists and LETs. Thus, we can skip updating boundaries at all steps other than the first step.

Others mainly include the data copies. The number of data copies also reduce if we use the

**Table 1.** Break down

Operation	first step	64 averaged	speedup
exchange Particles	0.308 (18%)	0.00481 (1.5%)	64.0
Local Tree construction	0.0568 (3.3%)	0.000888 (0.27%)	64.0
Local Tree update	0.0195 (1.1%)	0.0130 (4.0%)	1.5
LET construction	0.00416 (0.24%)	$6.50 \times 10^{-5}$ (0.20%)	64.0
LET communication	0.0238 (1.4%)	0.0128 (4.0%)	1.86
Global Tree construction	0.178 (10%)	0.0141 (4.4%)	12.6
Global Tree update	0.0273 (1.6%)	0.0165 (5.1%)	1.65
Interaction List construction	0.657 (38%)	0.0103 (3.2%)	64.0
Interaction calculation	0.285 (17%)	0.235 (73%)	1.21
Others	0.150 (8.8%)	0.0156 (4.8%)	9.62
Total	1.71	0.323	5.29

persistent list method.

## 6 Summary and Discussion

### 6.1 Real Size Ring Simulation

As we see in section 1, to investigate the ring structure, we need  $10^{16} - 10^{19}$  particle-steps. With our code, we can integrate about  $3.2 \times 10^6$  particles per second per process. In other words, to investigate planetary ring dynamics, we need  $8.7 \times 10^5 - 8.7 \times 10^8$  process hours. If we can use nearly full node of Sunway TaihuLight or other super computers with similar peak performance, the simulations would be finished within the reasonable time. In near future, we will perform these simulations.

### 6.2 Extension of Proposed Algorithms

Proposed algorithms are developed for the planetary ring simulations. However, we believe that some of them are also useful for other particle based simulations.

The persistent list method is based on the nature of the ring system which is the velocity dispersion of the system is very low so that the particle relative positions keep almost the same for a timestep. Thus we can use this methods for SPH (Smoothed Particle Hydrodynamics), MD (Molecular Dynamics) or DEM (Discrete Element Method) simulations.

This method is also useful  $N$ -body+SPH simulation such as galaxy formation simulations.

This is because the timestep of the simulation should be determined by SPH particles not by  $N$ -body particles with high velocity dispersion.

The super domain method (or introducing tree structure to the domains) would become necessary to simulate long-range force systems, if we want to use many processes. This is because the execution time for all-to-all communication increase at least linearly against the number of processes.

In this paper, we use only level-two tree structure. This is good enough for our aim. However, if we use more processes we might need to introduce more general tree structure to the domain decomposition. We will study it in near future.

The proposed load balancer for interaction calculations is also useful on other manycore processors. Since our algorithms is static, in contrast with a dynamic load balancer, there is no load balancing overhead during interaction calculation, which would increase as the number of cores. As an load balancing overhead, our algorithm requires to sort interaction groups. However, if we use the persistent list method, the sort is required only at the first step for multiple steps. In addition, the sort can be parallelized on all cores. Thus our load balancer could be better compared to other dynamic ones, if we use the persistent list method on manycore processors.

### 6.3 Summary

In this paper, we described the algorithms and performance of a highly efficient simulation code for self-gravitating planetary rings on the Sunway TaihuLight system. We mainly develop five new algorithms: 1) Persistently use the same interaction list for multiple timesteps. 2) Use the cylindrical coordinate for constructing the domain and the tree structure. 3) Counter rotate particles for decreasing communication costs for exchange particles. 4) Introduce super domains to remove all-to-all communication for exchange LET. 5) Introduce a load balancer to assign interaction calculations on cores to achieve a good load balance. We implement these algorithms to FDPS and we achieve 3.83 PFlops, or 31 % of the theoretical peak on 16384 processes (4096 nodes). It means we are ready to perform real size ring simulation. In near future, we will try to perform these simulations to investigate the formation and evolution of the planetary ring.

## Appendix 1 Force Kernel Tuning on SW21060

Since the force kernel is the most intensive part in  $N$ -body simulation, we need fast force kernel. In our code, different CPEs calculate different  $i$ -particle groups. At first, each CPE stores 256  $i$ -particles and 4  $j$ -particles to its local memory. Then CPE calculate forces on 256  $i$ -particles from 4  $j$ -particles. To hidden the latency of reading  $j$ -particles, during force calculation, next 4  $j$ -particles are stored with

DMA.

For tuning on the force kernel itself, we develop it in assembly language because the optimization by the compiler is limited. In addition, instruction set of Sunway 26010 processor does not include fast approximation for neither square root or reciprocal square root. So we implemented fast initial guess and high-order convergence iteration in software.

## **Appendix 2 Sort on SW21060**

The sorting in the particles frequently used in our code. For example for the tree construction, we sort the particles by their Morton key. In original implementation of FDPS, we use the radix sort for integer numbers. The radix sort is easily parallelized and is known one of the fastest sort on GPUs.

The bottleneck of the radix sort is the bandwidth of the main memory. The bandwidth of SW21060 processor is about ten times smaller than that of the current GPU, such as GTX1080. Thus the radix sort is not optimal choice on SW21060.

Instead of the radix sort, we used so-called sample-sort method. The steps of the sample sort is as follows.

1. Sample elements randomly and store them to the local memory.
2. Sort the samples by quick sort on single core.
3. Find the partition to split the sample into 64 segments equivalently and assign 64 segments to 64 CPEs one-by-one.
4. Store elements from original array to appropriate local memory.
5. Sort the elements by quick sort on each CPEs.

In this method, once we store elements to the local memory, CPEs do not need to access to the main memory, until the sort is done. Thus the main memory bandwidth is not serious issue.

## **References**

- Ballouz, R.-L., Richardson, D. C., & Morishima, R. 2017, AJ, 153, 146
- Barnes, J., & Hut, P. 1986, Nature, 324, 446
- Bédorf, J., Gaburov, E., Fujii, M. S., et al. 2014, Proceedings of the International Conference for High Performance Computing, Networking, Storage and Analysis, p. 54-65, 54
- Hamada, T., Narumi, T., Yokota, R., Yasuoka, K., Nitadori, K., & Taiji, M. 2009, Proceedings of the Conference on High Performance Computing Networking, Storage and Analysis, 62, 12
- Ishiyama, T., Nitadori, K., & Makino, J. 2012, Proceedings of the International Conference on High

Performance Computing, Networking, Storage and Analysis, 5, 1

Ishiyama, T. 2014, ApJ, 788, 27

Iwasawa, M., Tanikawa, A., Hosono, N., et al. 2016, PASJ, 68, 54

Makino, J. 2004, PASJ, 56, 521

Michikoshi, S., & Kokubo, E. 2017, ApJL, 837, L13

Portegies Zwart, S., & Bédorf, J. 2014, arXiv:1409.5474

Rein, H., & Latter, H. N. 2013, MNRAS, 431, 145

H. Rein & S.-F. Liu, 2012, A&A, 537, 128

Stadel, J. G. 2001, Ph.D. Thesis, 3657

Wisdom, J., & Tremaine, S. 1988, AJ, 95, 925

Zebker, H. A., Marouf, E. A., & Tyler, G. L. 1985, Icarus, 64, 531